PHYSICAL REVIEW B **94**, 020407(R) (2016)

Unconventional magnetism on a honeycomb lattice in α-$RuCl_3$ studied by muon spin rotation

F. Lang,[1,*] P. J. Baker,[2] A. A. Haghighirad,[1] Y. Li,[3] D. Prabhakaran,[1] R. Valentí,[3] and S. J. Blundell[1,†]

[1]*Oxford University Department of Physics, Clarendon Laboratory, Parks Road, Oxford, OX1 3PU, United Kingdom*

[2]*ISIS Facility, Rutherford Appleton Laboratory, Chilton, Oxfordshire OX11 0QX, United Kingdom*

[3]*Institut für Theoretische Physik, Goethe-Universität Frankfurt, 60438 Frankfurt am Main, Germany*

(Received 15 April 2016; published 14 July 2016)

Muon spin rotation measurements have been performed on a powder sample of α-$RuCl_3$, a layered material in which Ru ions are arranged on a honeycomb lattice and which previously has been proposed to be close to a quantum spin liquid ground state. Our data reveal two distinct transitions at 11 and 14 K, which we interpret as originating from the onset of three-dimensional order and in-plane magnetic order, respectively. We identify, with the help of density functional theory calculations, likely muon stopping sites and combine these with dipolar field calculations to show that the two measured muon rotation frequencies are consistent with two inequivalent muon sites within a zigzag antiferromagnetic structure proposed previously.

DOI: 10.1103/PhysRevB.94.020407

Solid-state systems with architectures that contain triangles or tetrahedra offer the possibility of realizing novel magnetically frustrated states, such as quantum spin liquids [1] or exotic topological phases [2]. One such candidate system for frustrated magnetism is α-$RuCl_3$, which adopts the honeycomb structure. It is thought to be a spin-orbit assisted Mott insulator [3,4], in which both the near two dimensionality of the separate honeycomb layers and bond-dependent interactions, which may embody Kitaev physics, are proposed to be major ingredients [5]. Unconventional excitations observed via Raman [6] and inelastic neutron scattering [7] have been presented as evidence that α-$RuCl_3$ may be close to a quantum spin liquid ground state. Various magnetic transitions have been reported in α-$RuCl_3$ with early studies pointing towards an antiferromagnetic transition with numerous reported temperatures of 13 K [8], 15.6 K [9], or even 30 K [10], while later investigations proposed a potential second transition around 8 K [11–13] thought to originate from low-moment magnetism. Recent neutron powder diffraction provided evidence for a single transition to a zigzag antiferromagnetic state with two-layer stacking at $T_N = 13$ K [14], though a later single crystal neutron study has proposed a single transition at 8 K to a three-layer stacking magnetic order in pristine single crystals and a change of T_c to 14 K upon mechanical deformation of the crystals [15]. These differences in observed properties could be due to the propensity of this compound to exhibit stacking faults between the weakly coupled honeycomb layers [14].

Positive muons as local magnetic probes present an ideal tool for detecting magnetic order and characterizing magnetic behavior, and have been extensively utilized in muon-spin rotation or relaxation (μ^+SR) studies of frustrated systems [16], and various layered magnets [17–19], including Na_2IrO_3 [20] which has a layered honeycomb structure similar to α-$RuCl_3$. Here, we present results from zero-field (ZF) μ^+SR investigations of α-$RuCl_3$ powder complemented by a theoretical analysis based on density functional theory (DFT) and dipolar field calculations. Below about 14 K our sample shows clear evidence for long-range magnetic order, with two muon precession signals resolvable at low temperature. However, there are clear indications of the higher frequency signal vanishing above a slightly lower temperature of about 11 K.

Polycrystalline samples of α-$RuCl_3$ were synthesized by vacuum sublimation from commercial $RuCl_3$ powder (Sigma Aldrich), which was sealed in a quartz ampoule ($p \approx 10^{-5}$ mbar) and placed in a three-zone furnace with a hot and cold end of 650 °C and 450 °C, respectively. Those temperatures were chosen in order to obtain phase-pure α-$RuCl_3$ (the β polytype transforms irreversibly into the α phase above 395 °C) and to keep the Cl_2 gas pressure in the ampoule below atmospheric pressure. The polycrystalline material harvested from the ampoule contained many platelike shiny crystals of hexagonal shape. X-ray diffraction confirmed the samples to be single phase and in agreement with the $C2/m$ structure [14,15] (see the Supplemental Material [21] for more details on the x-ray characterization).

We conducted ZF μ^+SR measurements of a powder sample of α-$RuCl_3$ on the EMU spectrometer at the ISIS muon facility, RAL (UK), as well as the GPS spectrometer at the Swiss Muon Source, PSI (Switzerland). Data were collected in the temperature range 1.5–40 K using ^{4}He cryostats. In a μ^+SR experiment spin-polarized muons are implanted into a sample, where they Larmor precess around the local magnetic field at the muon stopping site. By measuring the angular distribution of the decay product positrons the spin polarization can be tracked. In the case of long-range magnetic order, coherent magnetic fields at particular muon stopping sites within the unit cell lead to oscillatory signals with frequencies dependent on the local magnetic fields at each site. In μ^+SR impurity phases only contribute according to their volume fraction, and so the technique is an effective measure of intrinsic behavior.

Representative raw data obtained are plotted in Fig. 1(a) with Fourier transform spectra presented in Fig. 1(b). The measurements reveal oscillations below 14 K with two clearly separate frequencies at low temperatures around 1 and 2.5 MHz, resulting from two inequivalent muon stopping sites with local fields of 7.5 and 18.5 mT, respectively.

The μ^+SR data can be well fitted below 11 K with a sum of two oscillating functions $A_i \cos \omega_i t e^{-\lambda_i t}$, where the

*franz.lang@physics.ox.ac.uk
†s.blundell@physics.ox.ac.uk

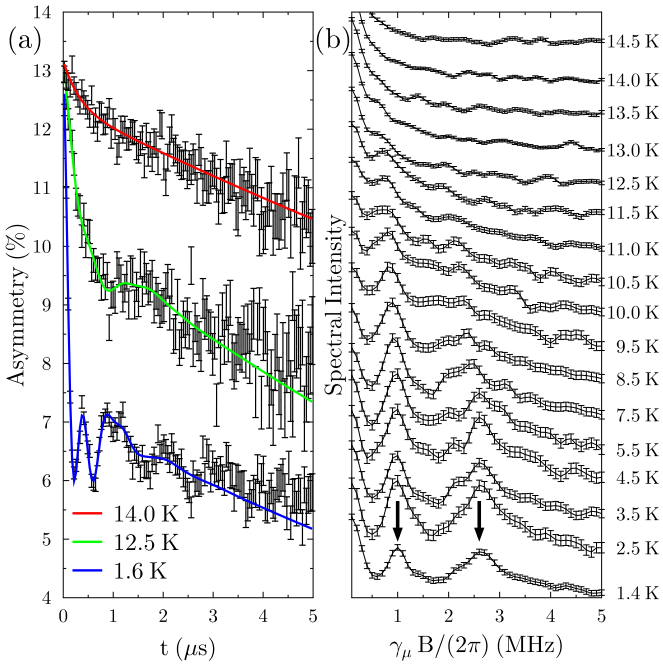

FIG. 1. Panel (a): Muon asymmetries at selected temperatures. Solid lines represent fits using two ($T \lesssim 11$ K) or one (11 K $\lesssim T \lesssim$ 14 K) oscillating components with a Lorentzian relaxation. Panel (b): Fourier transform spectra of the muon asymmetries (vertically displaced for clarity).

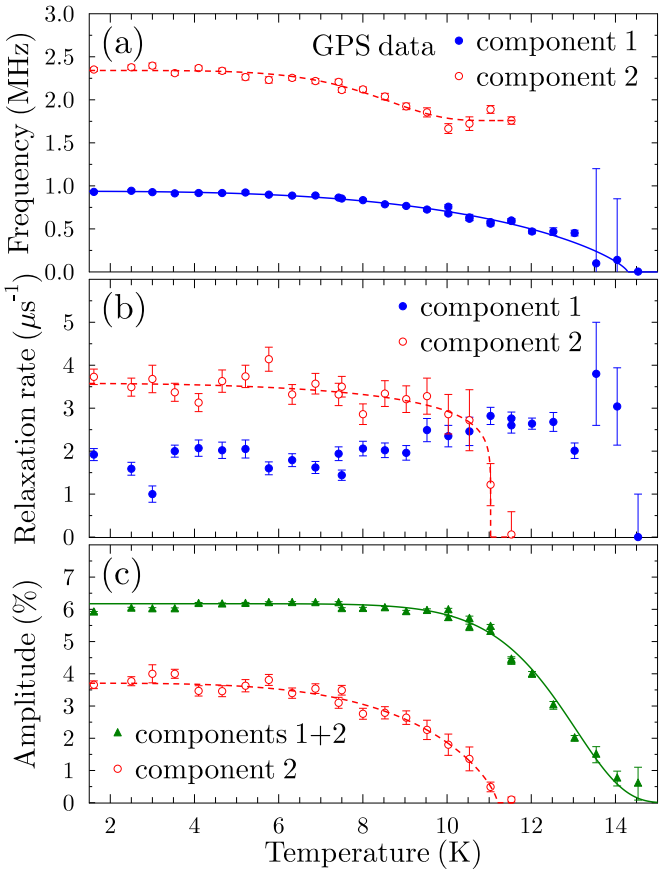

FIG. 2. Results of fitting two oscillation frequencies with Lorentzian relaxation to the muon asymmetry. The lines represent order parameter fits of the form $y^2 = y_0^2[1-(x/T_c)^\alpha]^\beta + c^2$.

exponentials allow for relaxation caused by slow dynamics of the magnetic moments. In addition, a very slowly relaxing background term $A_b e^{-\lambda_b t}$ is included to account for muons stopping in the sample holder. In the range 11 K $\lesssim T \lesssim$ 14 K only one oscillating component (plus background term) is required. Figure 2 presents the resulting frequencies ω_i, relaxation rates λ_i, and oscillation amplitudes of the precession signals for the data collected on the GPS spectrometer. The fits were performed in the time range $t < 3$ μs with a goodness of fit of χ^2=1.03 (5) per degree of freedom averaged over all fits. Essentially identical results were obtained on the same sample in a separate experiment using the EMU spectrometer, demonstrating reproducibility. The fitted parameters can be modeled with a phenomenological order parameter equation of the form $y^2 = y_0^2[1-(x/T_c)^\alpha]^\beta + c^2$ to give critical temperatures of 11.0(5) and 14.3(3) K for the high and low frequency components, respectively, and a volume fraction ratio of roughly 4:2. The presence of two μ^+SR precession signals necessitates two inequivalent muon stopping sites in the magnetic phase of our sample, whose origin we discuss later. We further note that the amplitude of the higher frequency falls to zero, even while its frequency is nonzero.

Further analysis requires the knowledge of the potential muon stopping sites. Therefore, we employ DFT calculations to map out the electrostatic Coulomb potential of α-$RuCl_3$ throughout its unit cell. The maxima of such a potential map have been a reliable approximation to the muon sites in previous more in-depth "DFT+μ" calculations, which also accounted for local distortions of the lattice caused by the muon presence [22–24].

We performed DFT calculations within the generalized gradient approximation [25] by employing the full potential linearized augmented plane wave basis as implemented in WIEN2K [26]. The $RK_{\max}$ parameter was set to 9 and we used a mesh of 800 **k** points in the first Brillouin zone. The electrostatic (Coulomb) potential was calculated from the converged electron density and the three-dimensional electrostatic potential maps were obtained with the XCRYSDEN package [27] and visualized with the VESTA software [28].

The Coulomb potential of α-$RuCl_3$ calculated via DFT is plotted in Fig. 3, with the global maximum of the potential chosen as the reference value. A large Coulomb potential corresponds to a low energy required to add a positive charge. Therefore, by considering regions of high electrostatic potential, and particularly local maxima, we can identify plausible regions for a muon to stop in. When additionally taking into account that we expect a μ^+ to implant near a Cl^- ion [21], we find four plausible muon site candidates, which are shown in Fig. 3 and summarized in Table I. These candidate sites are separated by up to 0.4 eV in their Coulomb potential values, with the origin (Mu1) being the lowest. While the muon will generally perturb its local environment, its effect is short ranged and significant only for the nearest-neighbor ions [22,23], and in the present case we anticipate only a small displacement of a nearest Cl^- ion and negligible effect on the magnetic moment carrying Ru^{3+} ions. As a result, we do

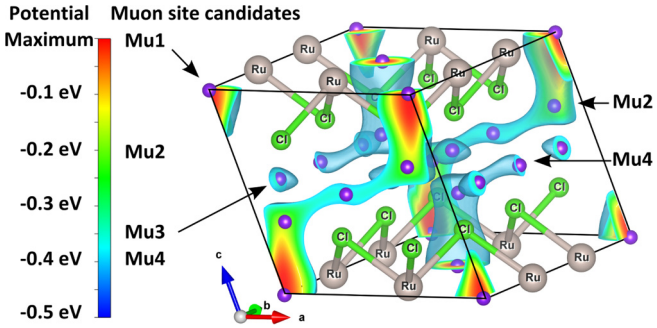

FIG. 3. Coulomb potential of α-$RuCl_3$ calculated via DFT. The blue isosurface plotted is at 0.4 eV below the maximum. The purple spheres indicate the muon site candidates we identified. Their labels are placed next to the color scale to indicate the approximate value of the potential at the sites.

not expect distortions to have a significant impact on the bulk magnetism probed in our μ^+SR measurement.

We now calculate the local magnetic field experienced by an implanted muon. This field is in general a sum of contributions due to dipolar couplings, demagnetizing and Lorentz fields, and hyperfine interactions. Since α-$RuCl_3$ orders antiferromagnetically the demagnetizing and Lorentz fields are zero. We expect the μ^+ to stop near Cl^- ions and thus direct overlap with any Ru^{3+} electron spin density will be tiny and so we neglect any hyperfine contribution [22,29]. Therefore, we focus on the dominant dipole field only, which for a muon at position $\boldsymbol{r}_\mu$ and magnetic moments $\boldsymbol{\mu}_i$ at $\boldsymbol{r}_i$ is given by

$$\boldsymbol{B}_{\rm dip}(\boldsymbol{r}_\mu) = \sum_i \frac{\mu_o}{4\pi|\Delta\boldsymbol{r}_i|^3}\left[\frac{3(\boldsymbol{\mu}_i\cdot\Delta\boldsymbol{r}_i)\Delta\boldsymbol{r}_i}{|\Delta\boldsymbol{r}_i|^2} - \boldsymbol{\mu}_i\right], \quad (1)$$

where $\Delta\boldsymbol{r}_i = \boldsymbol{r}_i - \boldsymbol{r}_\mu$.

There exists substantial knowledge about the magnetic structure of α-$RuCl_3$ based on neutron diffraction experiments. One neutron powder study provided evidence for a zigzag antiferromagnetic order within each Ru honeycomb layer with an additional antiferromagnetic stacking between the layers. The corresponding propagation vector is $\boldsymbol{k} = (0,1,0.5)$, and moreover the moments are constrained to lie in the ac plane and the lower limit of the moment size is $0.64(4)\mu_B$ [14].

TABLE I. Fractional coordinates of atoms and muon site candidates determined through DFT calculations. Abbreviations stand for Wyckoff position (WP) and site symmetry (SS). The fractional coordinates of α-$RuCl_3$ originate from Ref. [14] and are compatible with x-ray diffraction characterization [21].

Atom	WP	SS	x	y	z
Ru	$4g$	2	0	0.33441	0
Cl	$4i$	m	0.73023	0	0.23895
Cl	$8j$	1	0.75138	0.17350	0.76619
Mu1	$2a$	$2/m$	0	0	0
Mu2	$4i$	m	0.14	0	0.36
Mu3	$4g$	2	0	0.2	0.5
Mu4	$2d$	$2/m$	0.5	0	0.5

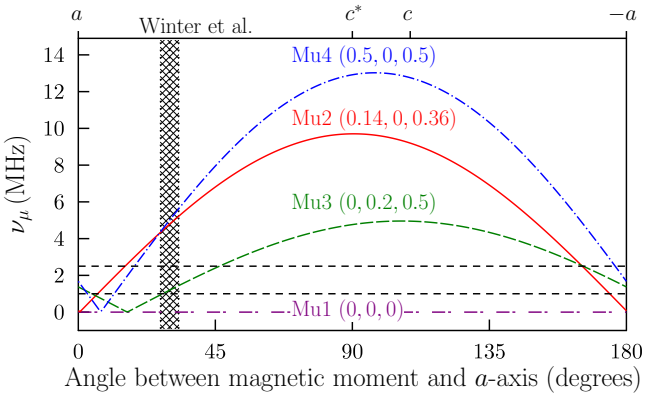

FIG. 4. Muon Larmor precession frequencies due to dipolar fields at the four muon site candidates as a function of the magnetic moment direction in the ac plane. Directions parallel to crystallographic axes are indicated at the top of the plot. The magnetic structure was taken to be the two-layer ordering proposed by Johnson *et al.* [14] and the approximate moment direction predicted by Winter *et al.* [30] has been marked. Horizontal dashed lines indicate the two measured frequencies.

However, another recent single crystal measurement proposed an alternative zigzag antiferromagnetic ordering with three-layer stacking [$\boldsymbol{k} = (0,1,1/3)$] in pristine single crystals with moments aligning in the ac plane in a spiral or collinear pattern [15]. Investigations using *ab initio* and model calculations also find an in-plane zig-zag antiferromagnetic order [30,31] and predict the magnetic moments to make an angle of $\approx 30^\circ$ with the ab plane [30,32].

Using the known crystal structure and the proposed two-layer magnetic ordering we computed the dipole field strength at the candidate muon sites obtained through DFT simulations. Figure 4 displays the resulting Larmor frequencies and how they change as a function of the magnetic moment direction within the ac plane. Note that the dipole field vanishes due to the local symmetry at candidate site Mu1, which is the electrostatically most favorable one. Figure 4 reveals that there is no single moment direction within the ac plane for which we obtain precession frequencies that agree with both the experimentally observed ones. We can improve our estimates by incorporating the fact that we expect the muon to form a bond with a nearby Cl^- ion of length $\approx$1.5 Å [21]. Our revised model considers the muon site to be displaced from our earlier candidate sites towards each of the nearest Cl^- ions. Figure 5 presents the resulting muon precession frequencies as a function of the magnetic moment direction. It shows that if we take the moment to be at $\approx 30^\circ$ with the ab plane [30] and small distortions towards the nearest neighbor Cl^- ions both the Mu1 and Mu3 site candidates are compatible with the experimentally observed frequencies. It should be noted that both Mu1 and Mu3 have six nearby Cl^- ions, four of which are at the $8j$ Wyckoff positions and two of which are at the $4i$ Wyckoff positions (see Table I). We also considered the effect of stacking faults at which the $RuCl_3$ layers are translated by $\pm\mathbf{b}/3$ [14]. We find that such faults can result in a lowering of the precession frequency from muons at the Mu1, Mu2, and Mu4 sites, but also different

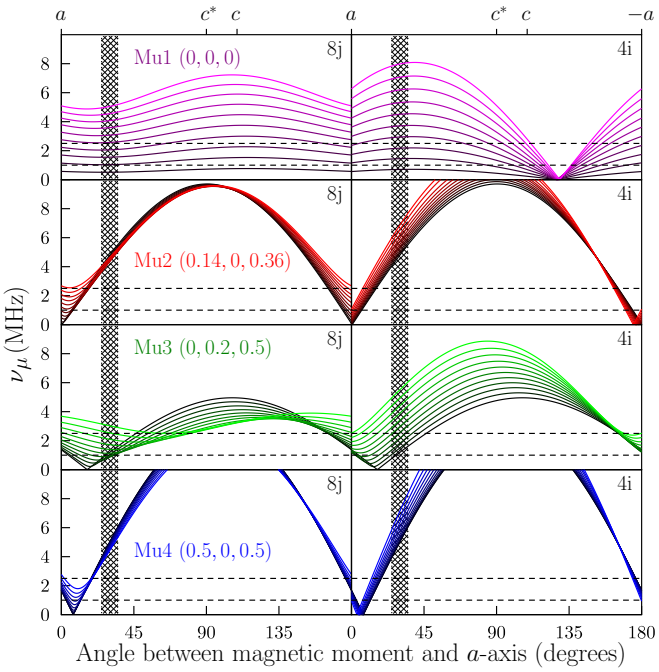

FIG. 5. Muon Larmor precession frequencies at the muon site candidates (black curves) and for ten positions (0.1 Å between each) along a straight line towards the nearest Cl^- ions (colored curves), as a function of the magnetic moment direction in the *ac* plane. Positions further away from the undistorted muon site candidates are displayed more colorfully. The left and right columns show distortions towards Cl^- ions on the 8*j* and 4*i* Wyckoff positions, respectively (see Table I). The magnetic structure was taken to be the two-layer ordering proposed by Johnson *et al.* [14]. Moment directions parallel to crystallographic axes are indicated at the top and the approximate angle predicted by Winter *et al.* [30] is marked by the dotted vertical lines. Horizontal dashed lines indicate the two measured frequencies.

symmetry-equivalent sites can become inequivalent which could be a source of broadening [21]. However, stacking faults only have a significant effect on the precession signals if the muon is directly adjacent to the fault [21], and so we conclude that our measured Larmor frequencies are not significantly affected by the stacking faults. In conclusion, the zigzag antiferromagnetic order with two-layer stacking proposed by Johnson *et al.* [14] is compatible with our μ^+SR measurements of α-$RuCl_3$ powder.

We considered two plausible scenarios that could explain the two observed frequencies and transitions. First, we investigated the possibility that there could be two distinct magnetic phases: one resulting from regular stacking of the layers and another from an alternative stacking proposed previously [15]. However, our test DFT calculations [21] showed this second structure to be energetically less favorable, and moreover the second phase would not produce a distinct dipole-field signature from the first. Second, we explored the possibility that the known presence of stacking faults [14], which likely lead to a complex sequence of *interlayer* exchange interactions, could hinder the establishment of long-range order along k_z. Our simulations [21] show that a site near Mu1 is relatively insensitive to the magnetic configuration along k_z. Thus, if $k_z = 0.5$ order only locked in below 11 K, a muon at this site would not be affected and would produce a precession signal all the way up to 14 K. However, a Mu2 or Mu3 site is found to be more sensitive to the interlayer magnetic configuration and would detect a range of frequencies if $k_z = 0.5$ order is not established. Such a site could plausibly give rise to the higher frequency signal that only sets in below 11 K. This second scenario is consistent with our experimental observations. Within this picture the structural stacking faults alter the local interlayer hopping channels, allowing adjacent Ru planes to align either ferro- or antiferromagnetically dependent on the local structure. This structure-induced modulation of the interlayer coupling is expected to hinder the growth of interlayer correlations, thereby suppressing the onset temperature of three-dimensional order below the point at which substantial static correlations within the layers develop.

We repeated the dipole field analysis for the magnetic ordering with three-layer stacking that Cao *et al.* have proposed for pristine single crystals of α-$RuCl_3$ [15]. While the resulting precession frequencies are all of the same order of magnitude as the experimentally observed ones, in general the three-layer stacking leads to more than two observable frequencies to be expected, unless the frequencies due to muons stopping in the different layers and near the two types of Cl^- ions are equal because of the symmetry of the muon sites [21]. We conclude that the magnetic ordering with three-layer stacking is unlikely to be compatible with our powder results, though we cannot rule out their applicability to the single crystal samples of Ref. [15].

In conclusion, we have conducted μ^+SR measurements of a powder of α-$RuCl_3$ and confirmed a transition to long-range magnetic order below 14.3(3) K, with a second transition at 11.0(5) K. Using DFT calculations we identified candidates for the muon stopping site and analyzed the muon precession frequencies due to dipolar couplings at these sites, using two zigzag antiferromagnetic structures proposed by recent powder and single crystal neutron diffraction studies and *ab initio* calculations. After examining a number of possible scenarios, we find that our results are consistent with a two-layer ordering proposed by Johnson *et al.* [14]. We suggest an interpretation of our two transitions based on an intermediate temperature regime where static two-dimensional intralayer correlations are largely established, but interlayer correlations are not yet significant, with full three-dimensional order only operative below the lower transition. This is somewhat similar to a state proposed to exist in frustrated triangular Ising antiferromagnets [33].

This work is supported by EPSRC (UK) Grants No. 1380739 and No. EP/M020517/1. Y.L. acknowledges support through a China Scholarship Council (CSC) Fellowship. R.V. thanks the Deutsche Forschungsgemeinschaft (DFG) for funding through Grant No. SFB/TR49. We are also grateful for H. Lütkens providing technical assistance with the experiments at PSI, A. J. Steele for help with the dipole field calculations, R. Coldea for numerous insightful ideas and valuable conversations, and W. Hayes, R. Johnson, and S. Winter for useful discussions.

[1] L. Balents, Nature **464**, 199 (2010).
[2] G. Jackeli and G. Khaliullin, Phys. Rev. Lett. **102**, 017205 (2009).
[3] X. Zhou, H. Li, J. Waugh, S. Parham, H.-S. Kim, J. Sears, A. Gomes, H.-Y. Kee, Y.-J. Kim, and D. Dessau, arXiv:1603.02279.
[4] I. Pollini, Phys. Rev. B **50**, 2095 (1994).
[5] K. W. Plumb, J. P. Clancy, L. J. Sandilands, V. V. Shankar, Y. F. Hu, K. S. Burch, H.-Y. Kee, and Y.-J. Kim, Phys. Rev. B **90**, 041112 (2014).
[6] L. J. Sandilands, Y. Tian, K. W. Plumb, Y.-J. Kim, and K. S. Burch, Phys. Rev. Lett. **114**, 147201 (2015).
[7] A. Banerjee, C. A. Bridges, J.-Q. Yan, A. A. Aczel, L. Li, M. B. Stone, G. E. Granroth, M. D. Lumsden, Y. Yiu, J. Knolle, S. Bhattacharjee, D. L. Kovrizhin, R. Moessner, D. A. Tennant, D. G. Mandrus, and S. E. Nagler, Nat. Mater. **15**, 733 (2016).
[8] J. M. Fletcher, W. E. Gardner, A. C. Fox, and G. Topping, J. Chem. Soc. A, 1038 (1967).
[9] Y. Kobayashi, T. Okada, K. Asai, M. Katada, H. Sano, and F. Ambe, Inorg. Chem. **31**, 4570 (1992).
[10] J. M. Fletcher, W. E. Gardner, E. W. Hooper, K. R. Hyde, F. H. Moore, and J. L. Woodhead, Nature **199**, 1089 (1963).
[11] M. Majumder, M. Schmidt, H. Rosner, A. A. Tsirlin, H. Yasuoka, and M. Baenitz, Phys. Rev. B **91**, 180401 (2015).
[12] J. A. Sears, M. Songvilay, K. W. Plumb, J. P. Clancy, Y. Qiu, Y. Zhao, D. Parshall, and Y.-J. Kim, Phys. Rev. B **91**, 144420 (2015).
[13] Y. Kubota, H. Tanaka, T. Ono, Y. Narumi, and K. Kindo, Phys. Rev. B **91**, 094422 (2015).
[14] R. D. Johnson, S. C. Williams, A. A. Haghighirad, J. Singleton, V. Zapf, P. Manuel, I. I. Mazin, Y. Li, H. O. Jeschke, R. Valentí, and R. Coldea, Phys. Rev. B **92**, 235119 (2015).
[15] H. B. Cao, A. Banerjee, J.-Q. Yan, C. A. Bridges, M. D. Lumsden, D. G. Mandrus, D. A. Tennant, B. C. Chakoumakos, and S. E. Nagler, Phys. Rev. B **93**, 134423 (2016).
[16] P. Carretta and A. Keren, in *Highly Frustrated Magnetism*, edited by C. Lacroix, P. Mendels, and F. Mila (Springer, New York, 2011), pp. 79–106.
[17] T. Lancaster, S. J. Blundell, P. J. Baker, M. L. Brooks, W. Hayes, F. L. Pratt, R. Coldea, T. Sörgel, and M. Jansen, Phys. Rev. Lett. **100**, 017206 (2008).
[18] P. A. Goddard, J. L. Manson, J. Singleton, I. Franke, T. Lancaster, A. J. Steele, S. J. Blundell, C. Baines, F. L. Pratt, R. D. McDonald, O. E. Ayala-Valenzuela, J. F. Corbey, H. I. Southerland, P. Sengupta, and J. A. Schlueter, Phys. Rev. Lett. **108**, 077208 (2012).
[19] J. L. Manson, T. J. Woods, S. H. Lapidus, P. W. Stephens, H. I. Southerland, V. S. Zapf, J. Singleton, P. A. Goddard, T. Lancaster, A. J. Steele, and S. J. Blundell, Inorg. Chem. **51**, 1989 (2012).
[20] S. K. Choi, R. Coldea, A. N. Kolmogorov, T. Lancaster, I. I. Mazin, S. J. Blundell, P. G. Radaelli, Y. Singh, P. Gegenwart, K. R. Choi, S.-W. Cheong, P. J. Baker, C. Stock, and J. Taylor, Phys. Rev. Lett. **108**, 127204 (2012).
[21] See Supplemental Material at http://link.aps.org/supplemental/10.1103/PhysRevB.94.020407 for details.
[22] J. S. Möller, P. Bonfà, D. Ceresoli, F. Bernardini, S. J. Blundell, T. Lancaster, R. De Renzi, N. Marzari, I. Watanabe, S. Sulaiman, and M. I. Mohamed-Ibrahim, Phys. Scr. **88**, 068510 (2013).
[23] F. R. Foronda, F. Lang, J. S. Möller, T. Lancaster, A. T. Boothroyd, F. L. Pratt, S. R. Giblin, D. Prabhakaran, and S. J. Blundell, Phys. Rev. Lett. **114**, 017602 (2015).
[24] J. Möller, Muon-spin relaxation and its application in the study of molecular quantum magnets, Ph.D. thesis, University of Oxford, 2013.
[25] J. P. Perdew, K. Burke, and M. Ernzerhof, Phys. Rev. Lett. **77**, 3865 (1996).
[26] P. Blaha, K. Schwarz, G. Madsen, D. Kvasnicka, and J. Luitz, *WIEN2k, An Augmented Plane Wave + Local Orbitals Program for Calculating Crystal Properties* (Karlheinz Schwarz, Techn. Universität Wien, Austria, 2001).
[27] A. Kokalj, J. Mol. Graphics Modell. **17**, 176 (1999).
[28] K. Momma and F. Izumi, J. Appl. Crystallogr. **41**, 653 (2008).
[29] J. S. Möller, D. Ceresoli, T. Lancaster, N. Marzari, and S. J. Blundell, Phys. Rev. B **87**, 121108 (2013).
[30] S. M. Winter, Y. Li, H. O. Jeschke, and R. Valentí, Phys. Rev. B **93**, 214431 (2016).
[31] H.-S. Kim, V. Shankar V., A. Catuneanu, and H.-Y. Kee, Phys. Rev. B **91**, 241110(R) (2015).
[32] J. Chaloupka and G. Khaliullin, Phys. Rev. B **92**, 024413 (2015).
[33] F. J. Burnell and J. T. Chalker, Phys. Rev. B **92**, 220417 (2015).